Nigerian Journal of Technology (NIJOTECH)
Vol. 44, No. 1, March, 2025, pp.123 - 132
www.nijotech.com

Print ISSN: 0331-8443
Electronic ISSN: 2467-8821
https://doi.org/10.4314/njt.v44i1.14

EFFECT OF ZINC OXIDE, MANGANESE DIOXIDE NANOPARTICLES AND THEIR BLENDS ON YIELD AND QUALITY OF BIOETHANOL PRODUCED FROM CO-FERMENTATION OF BANANA AND POTATO PEELS

AUTHORS:
B. B. Uzoejinwa[1,*], A. O. Ezeama[2], C. L. Anioke[3], V. Ogwo[4], C. P. Ifeanyi-Obiorah[5] and C. M. Obiora[6]

AFFILIATIONS:
[1,2,4,5,6]Department of Agricultural and Bioresources Engineering, University of Nigeria, Nsukka
[3]Department of Electronic and Computer Engineering, University of Nigeria, Nsukka

***CORRESPONDING AUTHOR:**
Email: benjamin.uzoejinwa@unn.edu.ng

ARTICLE HISTORY:
Received: 08 August, 2024.
Revised: 23 January, 2025.
Accepted: 05 February, 2025.
Published: 14 April, 2025.

KEYWORDS:
Bioethanol production, Nanoparticles effect, Co-fermentation, Enhanced yield and quality.

ARTICLE INCLUDES:
Peer review

DATA AVAILABILITY:
On request from author(s)

EDITORS:
Chidozie Charles Nnaji

FUNDING:
None

Abstract

Effect of zinc oxide (ZnO) nanoparticles (NPs), manganese dioxide (MnO_2) NPs and their blends on the yield and quality of bioethanol produced from co-fermentation of banana and potato wastes has been investigated. Thus, in this study, ZnO, MnO_2 NPs and their novel blend were synthesized, characterized and employed as additives to the fermentation processes, and their effects on the yield and quality of bioethanol produced from various blends of the organic wastes were evaluated. Potato peels (PP) and banana peels (BP) were collected and prepared for sample characterization. Prepared samples were then pretreated using acid pretreatment method before enzymatic hydrolysis, co-fermentation and products analyses were carried out. Series of experiments were carried out using the feedstock blends: 100 wt.%BP: 0 wt.%PP, 30 wt. %BP: 70 wt.%PP, 70wt.%BP: 30 wt.%PP, 50 wt. %BP: 50 wt.%PP and 0 wt. %BP: 100 wt.%PP. The ZnO, MnO_2 and ZnO+MnO_2 NPs were added to the feedstock blends, and the blends without nanoparticles served as control samples. Study results unveiled that the highest yield of bioethanol (29.72g/l) was obtained from the sample blend, 100wt%BP + 0wt.%PP treated with ZnO NPs, and this was followed by 28.52g/l of bioethanol obtained from 50wt.%BP + 50wt.%PP sample blend treated with ZnO and ZnO +MnO_2 NPs. It was also observed that the amount of bioethanol produced from addition of ZnO NPs to samples is higher than those produced from control samples as well as from samples treated with MnO_2 and ZnO +MnO_2 NPs. This may be because ZnO acts as a better catalyst, positively enhancing the enzymatic activity which accelerates the conversion of sugars into ethanol than MnO_2 NPs. Product analysis results further unveiled the effect of the nanoparticles on the quality of bioethanol produced. Results of this study could enhance sustainability and economic viability of bioethanol production from organic wastes using nanoparticles.

1.0 INTRODUCTION

Due to depletion of fossil fuels and resultant global warming, researchers are exploring alternatives and eco-friendly fuel options, with biofuels being one of them. Besides being carbon neutral, biofuels are globally and domestically available for energy security [1], [2], [3]. Bioethanol is a clean and sustainable energy source often made by fermenting organic materials, mainly sugary or starchy crops like corn, sugarcane and wheat. The US, Brazil, the European Union, China and Canada are the top global bioethanol producers, with the US using corn and Brazil using sugarcane as feedstock [1]. The current feedstock situation presents a risk to food security due

HOW TO CITE:
Uzoejinwa, B. B., Ezeama, A. O., Anioke, C. L., Ogwo, V., Ifeanyi-Obiorah, C. P., and Obiora, C. M. "Effect of Zinc Oxide, Manganese Dioxide Nanoparticles and their Blends on Yield and Quality of Bioethanol Produced from Co-Fermentation of Banana and Potato Peels", *Nigerian Journal of Technology*, 2025; 44(1), pp. 123 – 132; *https://doi.org/10.4314/njt.v44i1.14*

to the increasing global population and the decrease in available arable land owing to rapid urbanization. Consequently, relying on food-based biofuel production is not a sustainable solution as it could result in higher crop prices or food insecurity [4], [5], [6]. However, a vast number of agricultural residues or lignocellulosic wastes are available, amounting to millions of tons. Unfortunately, there are no economically and environmentally feasible technologies currently accessible for converting these residues into useful products [7].

Besides, to enhance bioethanol yield and quality, the combination of distinct organic wastes through co-fermentation has been recommended. This procedure can amplify the variety of microorganisms in the fermentation process, leading to improved fermentation efficiency and higher bioethanol production. Likewise, the utilization of nanoparticles as an additive has also been proposed. Nanoparticles have the potential to act as a catalyst, augmenting the fermentation rate, and elevating bioethanol yield and quality [8], [9]. Various types of nanoparticles, including silver, titanium dioxide, graphene oxide and zinc oxide, have undergone test to determine their effectiveness in promoting bioethanol production [10], [11], [12], [13]. For example, Gupta and Chundawat [14] investigated the enhancement of bioethanol production from rice straw using ZnO nanoparticles, as a catalyst, which was biologically synthesized with *fusarium oxysporum*. The results showed a significant increase in ethanol yield using a certain concentration range during fermentation. Attia et al. [15] conducted a study on production of bioethanol from peels of potatoes using *saccharomyces cerevisiae* treated with ZnO/g-C_3N_4 and ZnO nanoparticles. The results showed that the method increased the yield of bioethanol with a shorter period of hydraulic retention time. Koppram et al. [16] investigated the co-fermentation and simultaneous saccharification of corncobs for production of bioethanol. They employed seven different recombinant xylose utilizing *Saccharomyces cerevisiae* strains and evaluated their fermentation performance using the hydrolysates of steam-pretreated corncobs. The result reported improved bioethanol yield but could be enhanced with pre-fermentation and a feed of substrate and enzymes.

Likewise, the effect of the nanoparticle (nickel oxide (NiO)) on production of bioethanol was investigated by Nduka et al. [17] using the substrates of banana peels. The researchers recorded that the addition of NiO NPs in the process enhanced the amount of bioethanol produced by a factor of two, which unveiled that the addition of the nanoparticle (NiO) could serve as a suitable biocatalyst in the production of bioethanol from waste organic materials. Another study, conducted by Sanusi et al. [18], examined the effect of the nanoparticle (Fe_3O_4) on bioethanol produced from the hydrolysates of banana peels using *Saccharomyces cerevisiae BY4743*. It was also observed that the metallic oxide nanoparticles enhanced the bioethanol production, with a maximum bioethanol yield of 0.26 g/g, glucose utilization of 99.95%, fermentation efficiency of 51%, bioethanol concentration of 5.24 g/L and 0.72 g/L/h maximum rate of production. Thus, the application of nanoparticles in bioethanol synthesis has greatly revolutionized the fermentation technology of converting carbohydrate-rich biomass into biofuels by significantly reducing the technical glitches and high costs associated with it through enhancement of the surface activity and selectivity involved in the process. As a result of this development, the application of nanoparticles in bioethanol synthesis is currently one of the most recent trends in bioethanol production [14], [17], [18].

However, to this extent, no study has investigated the integration of zinc oxide and manganese dioxide nanoparticles in the production of bioethanol from blends of organic wastes. Thus, in this study, ZnO, MnO_2 NPs and their novel blend were synthesized and characterized, the synthesized nanoparticles were employed in production of enhanced bioethanol, effects of the synthesized nanoparticles on the yield and quality of bioethanol produced from various blends of banana and potato wastes substrates were also investigated, and finally, samples of bioethanol produced were characterized to further unveil the extent of the effects of the applied synthesized nanoparticles. Results of this study would not only provide valuable information for developing an effective strategy for production of enhanced bioethanol but will also serve as an efficient method for resources recycling and wastes management as well as for enhancement of the sustainability and economic viability of bioethanol production from various blends of banana and potato wastes.

2.0 MATERIALS AND METHODS

2.1 Collection of Banana and Potato Peels

Potato and banana peels were collected from local potato fryer vendors and fruit sellers in Nsukka, Enugu State, Nigeria, respectively. The lignocellulosic materials were cleaned to reduce impurities before undergoing any process. The banana and potato peels were sun-dried for 5 days to final moisture contents of 6.57±0.4% and 5.86±0.2%,

respectively, and a milling machine was employed to grind the dried materials into a powdered form. Sieving was then performed with a 25nm sieve to obtain samples of homogenized particles with small sizes. Figure 1 presents the images of: (a) fresh banana peels, (b) fresh potato peels, (c) powered sun-dried banana peels and (d) powered sun-dried potato peels, respectively.

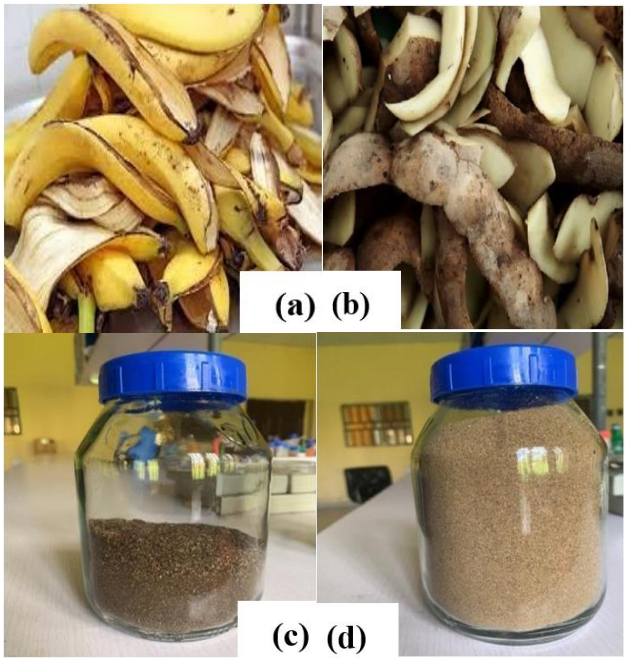

Figure 1: Images of: (a) fresh banana peels, (b) fresh potato peels, (c) powdered sun-dried banana peels and (d) powdered sun-dried potato peels

2.2 Characterization of Potato and Banana Peel Samples

Thermo-gravimetric and elemental analyses can be applied to any biological material to acquire the proximate and ultimate analyses parameters [19], [20]. In this study, these analyses were conducted on the two lignocellulosic materials, respectively. Moisture and ash levels were assessed using the air-oven and muffle furnace techniques, respectively, following the established procedures outlined by the Association of Official Analytical Chemists (AOAC) in 2000. For the determination of volatile matter, the American Society for Testing and Materials (ASTM) standards, specifically ASTM E870-82, were followed. The Nitrogen/Protein contents of both samples were determined using the Micro-Kjeldahl method as specified by AOAC (2000). To assess the Carbon content, the Wet method described by Walkley and Black in 1934 was employed [21]. Crude fiber and Crude fat contents were determined using experimental methods consistent with AOAC (2000) guidelines.

2.3 Synthesis of Nanoparticles

Materials and chemicals used for synthesis of the nanoparticles were obtained from Joechem Ventures, Nsukka, Enugu State, Nigeria, and National Centre for Energy Research Development (NCERD), University of Nigeria, Nsukka (UNN). For the synthesis of zinc oxide nanoparticles, 675 ml of 0.4M potassium hydroxide (KOH) was stirred for 5 minutes at room temperature. After, it was slowly added into 675ml of 0.2M zinc nitrate hexahydrate ($Zn(NO_3)_2.6H_2O$) solution at room temperature under vigorous stirring, which resulted in formation of a white suspension. The product was left undisturbed for 24 hours after which it was decanted and centrifuged. The white product was washed three times with distilled water and thereafter washed with ethanol. It was dried at 80°C, grinded, and calcined in the muffle furnace at 500°C for 3 hours. The resulting nanoparticles weighed 9.13g. For synthesis of manganese dioxide nanoparticles, 100ml of 0.4M glycerol solution was added drop-wise into 200ml of 0.3M potassium permanganate ($KMnO_4$) solution under vigorous stirring with a digital magnetic stirrer (with digital temperature display, speed-adjusting power of 200W, and maximum mixing capacity of 1000ml) for 20 minutes at room temperature to ensure uniform distribution of the reactants and reaction conditions. The resulting gel was kept undisturbed for 24 hours. After which it was decanted and centrifuged several times to remove excess K^+ ions. The solid was dried in an oven at 80°C. The dried manganese dioxide was crushed to fine particles. Crushed nanoparticles were calcined at 700°C for 6 hours and the resultant weight is 5.53g.

2.4 Pretreatment of the Samples

10g of each of the sample blends (100 wt.%BP: 0 wt.%PP, 30 wt. %BP: 70 wt.%PP, 70wt.%BP: 30 wt.%PP, 50 wt. %BP: 50 wt.%PP and 0 wt. %BP:100 wt.%PP) was pretreated with 0.5% H_2SO_4 in 40 ml of distilled water at 100°C for 20 minutes in a heating mantle to reduce the density, rigidity and crystalline structure of cellulose into easily fermentable sugars via hydrolysis. The solid residues were washed with deionized water to a neutral pH. The solutions with 4 or less were neutralized using 5% NaOH to a pH range of 5 to 6, and then transferred to an airtight bottle in preparation for hydrolysis.

2.5 Simultaneous Saccharification and Fermentation

Polysaccharides in the processed lignocellulosic biomass were hydrolyzed into individual monosaccharide components to enhance the fermentation process. Simultaneous saccharification

and fermentation (SSF) was carried out as described by Lavudi et al. [22]. For the Basal media preparation, a composition of 1.2g $NaNO_3$, 1.4g $(NH_4)SO_4$, 3.0g KH_2PO_4, 6.0g K_2HPO_4, 0.2g $MgSO_4.7H_2O$, 0.1g $CaCl_2$, 0.1g $MnSO_4.H_2O$, 0.1g $ZnSO_4.7H_2O$, 1.4g urea, 1% yeast extract, and 2% peptone were meticulously combined in 500 ml of distilled water, and the volume was adjusted to 1000 ml. The pH of the media was adjusted to a range of 5.5 to 6.0, and then the media was subjected to autoclaving at 121°C and 15 psi for 15 minutes. For post-autoclaving, 5% dextrose sugar was introduced into the media. Subsequently, 100 ml of the prepared media was dispensed into individual 250 ml flasks containing pretreated samples. Each of these flasks was then inoculated with 100 µl of *cellulase* under sterile conditions. After 72 hours, 2.5ml of *S. cerevisiae* was introduced into the control samples as well as the samples treated with ZnO, MnO_2, and ZnO + MnO_2, respectively, to initiate the fermentation process. 0.5g of ZnO, MnO_2, and ZnO + MnO_2 (at the ratio of 1:1) nanoparticles were added into the prepared samples, consecutively. The bottles were then left to incubate for an additional 72 hours at 28°C. Samples were filtered to separate the solid substrate from the liquid portion. Ethanol samples were obtained by subjecting the separated liquid to distillation at a temperature of 78.37°C (Figure 2).

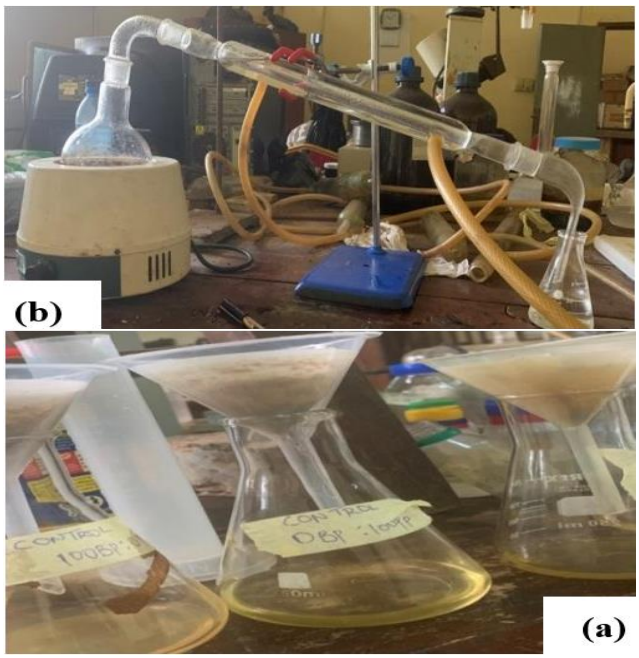

Figure 2: Experimental setup for: **(a)** the filtration process and **(b)** the distillation process

2.6 Product Analysis

The produced bioethanol was characterized to determine its fundamental properties, including density, flash point, viscosity, specific gravity and refractive index. The characterization and other research activities were carried out at NCERD, UNN following the ASTM set standards.

3.0 RESULTS AND DISCUSSIONS

3.1 Characterization Results

The results of the proximate, ultimate and composition analyses of the biomass samples are shown in Tables 1, 2 and 3, respectively. Banana peels had the highest moisture content of 12.87% when compared to potato peels with 5.61%, and also displayed higher values of crude fat, nitrogen, crude protein and volatile solid contents of 3.52%, 2.73%, 17.06%, and 88.02%, respectively. Banana peels have slightly higher fat content due to the presence of lipids in the peels cell membranes, but generally, the fat content in both peels is relatively low. Both banana and potato peels contain some amounts of proteins, but the protein content in banana peels tends to be slightly higher due to the presence of more amino acids in the plant tissues, though they are not a primary source of protein in the human diet [2]. Banana peels have a higher content of volatile compounds because they contain a variety of volatile compounds that contribute to their characteristic aroma and flavour. However, ash content was highest in potato peel (8.38%) than in banana peel (5.42%) owing to its higher content of minerals [23]. Besides, potato peels have higher crude fiber content (19.76%) and also higher content of carbohydrate compared to banana peels owing to their starchy tubers that store a significant amount of carbohydrates.

Table 1: Proximate analysis results of biomass samples

	Moisture content (%)	Volatile matter (%)	Ash content (%)	Crude fiber (%)	Crude fat (%)
Potato Peel	5.61	64.60	8.38	19.76	1.56
Banana Peel	12.87	88.02	5.42	17.20	3.52

Table 2: Ultimate analysis results of biomass samples

Parameters	Potato Peel	Banana Peel
Nitrogen content (%)	1.94	2.73
Carbon content (%)	44.08	35.65

Table 3: Composition analysis results of biomass samples

	Carbohydrate (%)	Protein (%)	Lignin (%)
Potato Peel	72.32	12.13	6.20
Banana Peel	61.13	17.06	6.98

3.2 Results of the Characterization of the Nanoparticles

Figure 3 shows the XRD characterization graphs of zinc oxide (ZnO) and manganese dioxide (MnO_2) nanoparticles (NPs), respectively. X-ray Diffraction

(XRD) analysis of nanoparticles is a common technique used to characterize the crystalline structure and phase purity of these nanoparticles. From Figure 3, the XRD patterns of ZnO NPs displayed the characteristic peaks at specific 2θ angles. These peaks correspond to the diffraction from the crystal lattice planes of the nanoparticles. Also, for the ZnO nanoparticles, the sharp diffraction peaks of the synthesized products indicate their good crystallinity [24]. The diffraction peaks in the XRD pattern exhibited the hexagonal crystal structure of ZnO NPs. This correlates with the outcome of other researchers like Hartanto et al. [25] who in their research on the synthesis of ZSM-5 noted that sharp peaks indicated that the ZSM-5 crystal has been formed. The results of XRD analysis of the MnO_2 NPs typically provide information about the crystalline structure, phase identification and other structural characteristics of the nanoparticles.

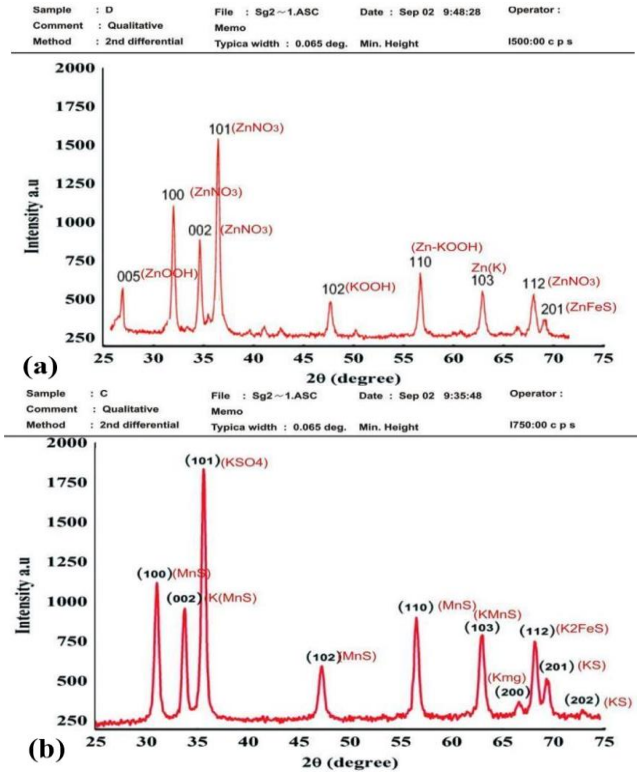

Figure 3: XRD graphs of: **(a)** ZnO NPs and **(b)** MnO_2 NPs

The XRD pattern displays characteristic peaks at specific 2θ angles. These peaks correspond to the diffraction from the crystal lattice planes of the MnO_2 NPs. Based on the peak positions and crystallographic data, the MnO_2 NPs exhibit a tetragonal or rutile crystal structure. A study conducted by Taranu et al.[26] on α-MnO_2 nanowire structure obtained hydrothermally (at low temperature) confirmed the tetragonal crystalline structure of α-MnO_2, that is several micrometers long. The observed peaks were compared to reference patterns in the International Centre for Diffraction Data (ICDD) database, and the pattern matched the MnO_2 phase.

3.3 Results of Quantity of Bioethanol Produced (Bioethanol Yield)

Figure 4 presents the quantities of bioethanol produced from all the sample blends. Collected distillates were quantified using a measuring cylinder and converted into amounts of bioethanol in grams per litre by multiplying the volume of collected distillates by density of bioethanol (0.8033 g/cm^3) [27]. From the figure, it can be observed that for all the samples, the highest yield of bioethanol (29.72g/l) was obtained from 100wt.%BP + 0wt.%PP sample blends treated with ZnO NPs, followed by the yields obtained from 50wt.%BP + 50wt.%PP sample blends treated with ZnO NPs and ZnO+MnO_2 NPs (at 1:1) which yielded 28.52g/l of bioethanol, respectively. The least yield of bioethanol was from the sample blend, 70wt.%BP + 30wt.%PP, treated with ZnO + MnO_2 NPs as well as from 50wt.%BP + 50wt.%PP sample blend treated with only MnO_2 NPs, of which both yielded 16.07g/l of bioethanol. Compared to the control samples, the addition of ZnO NPs increased the bioethanol yield in all the feedstock blends as it positively enhanced the activities of key enzymes involved in the fermentation process, which in turn accelerates the conversion of sugars into ethanol, leading to higher ethanol yields. From the results, it can also be deduced that ZnO NPs reacted positively to banana peels single feedstock blend than the potato peels single feedstock blend.

Banana peels are known to contain higher levels of cellulose and hemicellulose compared to potato peels which are the primary sources of fermentable sugars for bioethanol production. ZnO NPs typically have high surface area and porosity, which can enhance their adsorption capacity and catalytic activities, and hence interact more effectively with the cellulose and hemicellulose present in banana peels [28]. It can also be observed that the addition of MnO_2 NPs to the feedstock blends reduced the yields of bioethanol compared to the yields produced by the control sample blends and the reason may be because of the concentration of the nanoparticle as an excess of MnO_2 can disrupt the redox reaction equilibrium in the fermentation process. This imbalance can interfere with the metabolic pathways of the micro-organisms and hinder their ability to convert sugars into ethanol effectively. The only exception was the 70wt.%BP + 30wt.%PP feedstock blend treated with MnO_2 NPs, which yielded 23.30g/l of bioethanol with a slight increase compared to the same feedstock blend in the

control samples which yielded 21.69g/l of bioethanol. It was also observed that the addition of blends of ZnO and MnO_2 NPs in the feedstock samples of various blends increased the yields of bioethanol in 30wt.%BP + 70wt.%PP, 50wt.%BP + 50wt.%PP and 0wt.%BP + 100wt.%PP sample blends which gave 24.10g/l, 28.52g/l and 28.12g/l respectively compared to the same feedstock blends in the control samples which gave 23.30g/l, 17.67g/l and 27.51g/l respectively. However, it was also observed that the addition of blends of ZnO and MnO_2 NPs in the feedstock blends reduced the yields of bioethanol in 100wt.%BP + 0wt.%PP and 70wt.%BP + 30wt.%PP sample blends.

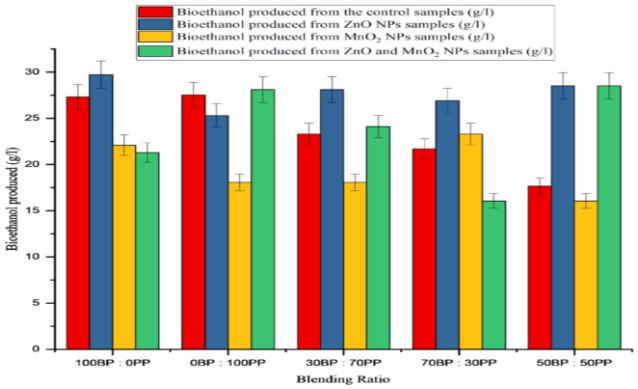

Figure 4: Chart showing the quantity of bioethanol produced from all sample blends

3.4 Product Analysis Results

The product analyses' results demonstrated how the incorporation of nanoparticles impacted the quality of bioethanol derived from the co-fermentation process of banana and potato peels. Fuel properties of the product (including density, flash point, viscosity, specific gravity and refractive index) were determined following ASTM procedures for petroleum products.

3.4.1 Density

The density of bioethanol produced was measured by hydrometer method (ASTM D1298 standard) using a Digital hydrometer (LCD English Display DH, BLS-1298, USA). From Figure 5, the sample blend (100BP:0PP) treated with ZnO NPs produced bioethanol with the highest density of 0.9989 g/cm^3, while the blend (0BP:100PP) treated with ZnO + MnO_2 NPs (at1:1 blending ratio) produced bioethanol with the least density (0.9733 g/cm^3). These values are higher than the 0.74 g/cm^3 reported by Kheiralla et al. [29] and also the ASTM standard for bioethanol density which is 0.789g/cm^3[30]. Bioethanol with a density in this range (0.9733 to 0.9989 g/cm^3) typically contains more energy per unit volume compared to pure anhydrous ethanol, leading to better fuel efficiency and increased energy output [30].. It can be well-suited for blending with gasoline to create ethanol-gasoline blends like E10 (10% ethanol). However, high density bioethanol may not perform optimally in engines calibrated to run on fuel meeting the ASTM set standards. It can lead to engine knocking, reduced fuel efficiency and even engine damage. Fuel systems, such as tanks, pipelines and dispensing equipment, designed for ethanol with ASTM compliant density may not handle high density bioethanol effectively. This can lead to equipment wear and increased maintenance costs. Besides, exceeding the ASTM set standard for bioethanol density could indicate the presence of impurities or contaminants like water in the bioethanol which can be corrosive to certain materials. These impurities may significantly affect fuel performance, engine operation and environmental emissions, necessitating further purification steps or quality control measures such as distillation or molecular sieving to eliminate water residues. The slightly higher density of bioethanol compared to the ASTM D287 standard may require adjustments to existing infrastructure, including storage tanks and transportation systems. This can be a disadvantage in terms of initial investment and adaptation.

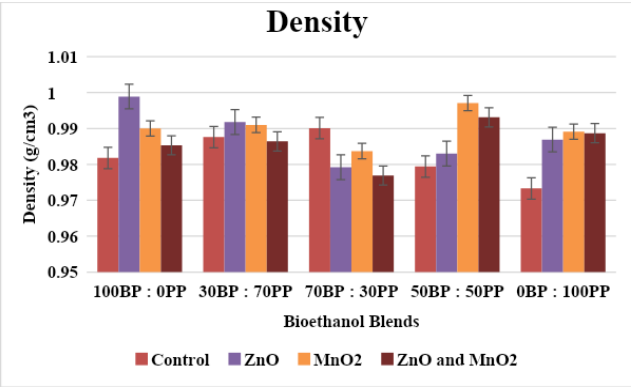

Figure 5: Densities of bioethanol produced under different treatments with nanoparticles

3.4.2 Flash point

Flash point of the produced bioethanol which signifies its flammability and potential for hazards during storage or transportation was measured using the Penskey-Marton apparatus [31]. Figure 6 reveals that the flash points of the produced bioethanol fall within the limit of 35-42°C, which significantly exceeds the ASTM-D93 set limit of 12-20°C. It can be deduced that the bioethanol produced is less flammable when compared to the ASTM-D93 set standard. A higher flash point indicates that the fuel is safe for handling, storage and transportation, even under mild temperature conditions. However, this can create safety concerns when it comes to engine operation. In an engine, the fuel must ignite readily to ensure efficient combustion. High flashpoint bioethanol may

not ignite easily in the engine, leading to poor combustion and potentially engine damage. Engines are designed to work with fuels that have specific ignition characteristics. If the fuel flash point is significantly higher than expected, it can lead to issues like misfiring, reduced power and poor fuel efficiency.

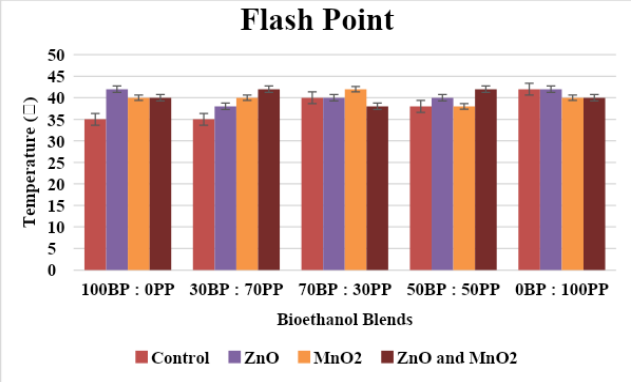

Figure 6: Flash points of bioethanol produced under different treatments with nanoparticles

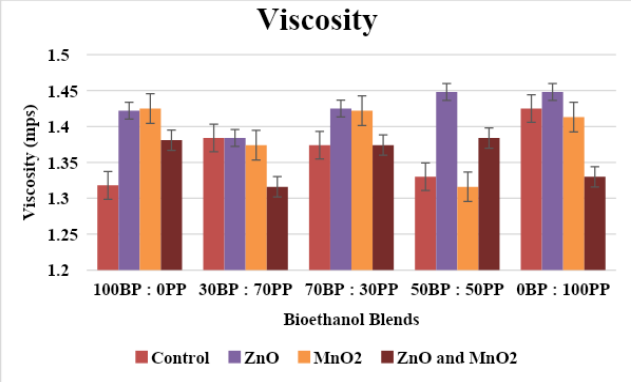

Figure 7: Viscosities of bioethanol produced under different treatments with nanoparticles

3.4.3 Viscosity

The viscosities of the produced bioethanol were determined using the viscometer (Ubbeholde viscometer 7143, India) according to the ASTM D445–06 standard method. Viscosities of the produced bioethanol at 20°C fall within the range of 1.32-1.45 millipascal-seconds (mPas) (Figure 7). Importantly, this range is within the ASTM D445 set limit of 1.10 to 1.5 mPas. The highest viscosity (1.45 mPas) was recorded with the feedstock blending ratios of 50wt.%BP + 50wt.%PP and 0wt.%BP + 100wt.%PP treated with ZnO NPs, and the least viscosity (1.316) was recorded with 30wt.%BP + 70wt.%PP and 50wt.%BP + 50wt.%PP blends treated with MnO_2 and ZnO + MnO_2 NPs, respectively. Bioethanol viscosity that is higher than the ASTM D445 standard can hinder the proper atomization of the fuel in engines leading to inefficient combustion and incomplete fuel mixing with air as well as a potential increase in emissions. In cold weather, the produced bioethanol can cause clogging of fuel filters and reduce the engine performance. These results agree with other results in the literature that nanoparticles addition improve the flash point, fire point, kinematic viscosity and other properties, based on their dosage [12], [13].

3.4.4 Specific gravity

The specific gravities of the samples of bioethanol produced from the various feedstock blends were determined using the Digital density meter (DDM 2910, USA) in accordance with the ASTM D4052–16 method. The specific gravities of the produced bioethanol (Figure 8) can be observed to be within the range of 0.973-0.999. It is worth noting that this range is higher than the ASTM standard value of 0.781. Specific gravity that is above this limit may affect the stability of ethanol-gasoline blends, the engine performance and may require adjustments in the blending ratios or engine settings to maintain optimal performance. In addition, specific gravity higher than this limit corresponds to high energy content per unit volume, resulting in better fuel efficiency and increased energy output when used as fuel. However, bioethanol with higher specific gravity may necessitate modifications to the existing fuel infrastructure, storage tanks and transportation systems to ensure proper handling and storage.

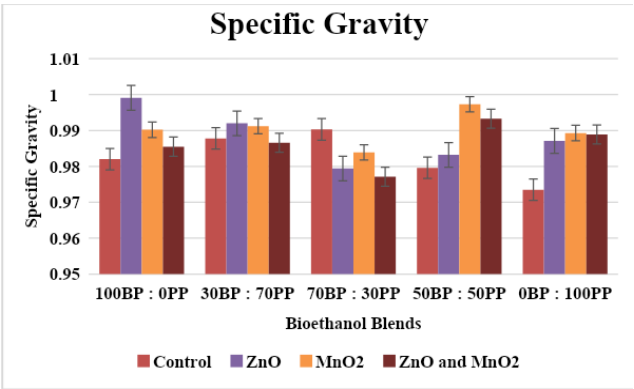

Figure 8: Specific gravities of bioethanol produced under different treatments with nanoparticles

3.4.5 Refractive index

The refractive indices of the produced bioethanol samples were obtained using a digital handheld refractometer (DHR Misco PA202, USA) following the ASTM procedure. Highest value of the refractive index (1.3547) was observed with the bioethanol produced from the 0wt.%BP + 100wt.%PP blend treated with MnO_2 NPs, and the lowest refractive index (1.353) was observed by treating the same blend with ZnO + MnO_2 NPs (Figure 9). The refractive

indexes of the bioethanol produced range from 1.3533 to 1.3547 which is close to the ASTM D1218/12 standard value of 1.362. This slightly higher refractive index could indicate the presence of impurities or variations in the chemical compositions of the bioethanol. Deviations in the refractive index may prompt additional quality control measures, which can increase production costs and complexity.

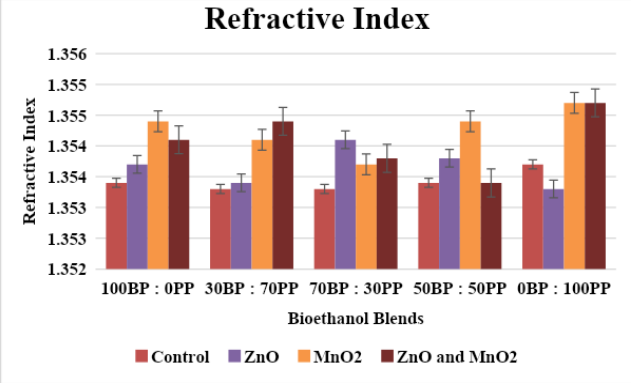

Figure 9: Refractive indexes of bioethanol produced under different nanoparticles treatments

4.0 CONCLUSION

Thus, this study has investigated the effect of the nanoparticles (ZnO, MnO_2, and their novel blend) on the yield and quality of bioethanol produced from co-fermentation of banana and potato peels using the feedstock sample blending ratios:. 100 wt.%BP: 0 wt.%PP, 30 wt. %BP: 70 wt.%PP, 70wt.%BP: 30 wt.%PP, 50 wt. %BP: 50 wt.%PP and 0 wt. %BP: 100 wt.%PP. The study results unveiled that the sample blend, 100wt%BP + 0wt.%PP + ZnO NPs, gave the highest yield of bioethanol of 29.72g/l, and this was followed by 28.52g/l of bioethanol obtained from the sample blend, 50wt.%BP + 50wt.%PP, with the addition of ZnO and ZnO + MnO_2 NPs, respectively. The results of the study also revealed that the amount of bioethanol produced from addition of ZnO nanoparticles to samples is higher than those produced from the control samples as well as samples treated with MnO_2 and ZnO + MnO_2 NPs. This observation may be attributed to the catalytic nature of the ZnO, which positively enhanced the enzymatic activity accelerating the conversion of sugars into ethanol than the MnO_2 nanoparticles. The results of product analyses performed also further unveiled the effect of the nanoparticles on the quality of the bioethanol produced. Thus, the results of this study could improve the sustainability and economic viability of bioethanol production from organic wastes using nanoparticles.

REFERENCES

[1] Akhtar, E. T. "Biofuels: A renewable solution for energy security and climate change mitigation", *SSRN Electron. J.*, 2023, doi: 10.2139/ssrn.4475528.

[2] LMC International, "Economic Impact of Biodiesel on the US Economy 2022: Main Report," *Clean Fuel Alliance America*, Nov. 2022. Accessed: Feb. 27, 2024. [Online]. Available: https://cleanfuels.org/wp-content/uploads/LMC_Economic-Impact-of-Biodiesel-on-the-US-Economy-2022_Main-Report_November-2022.pdf.

[3] Ogbeide-Igiebor, V., Ozigis, I. I. I., and Nasir, L. L. M. "Characterization of petrol, ethanol and spent engine oil blends for two-stroke single - cylinder spark - ignition engine", *Nigerian Journal of Technology*, vol. *43*, no 3, pp 471-478, Sept. 2024, doi: https://doi.org/10.4314/njt.v43i3.9.

[4] Epa, U. S. "Economics of Biofuels," *United States Environmental Protection Agency*, Accessed: Feb. 27, 2024. [Online]. Available: https://www.epa.gov/environmental-economics/economics-biofuels

[5] Vellakkal, S., Fledderjohann, J., Basu, S., Agrawal, S., Ebrahim, S., Campbell, O., Doyle, P., and Stuckler, D. "Food Price Spikes Are Associated with Increased Malnutrition among Children in Andhra Pradesh, India", *J. Nutr.*, vol. 145, no. 8, pp. 1942–1949, Aug. 2015, doi: 10.3945/jn.115.211250.

[6] Bušić, A., Marđetko, N., Kundas, S., Morzak, G., Belskaya, H., Šantek, M. I., Komes, D., Novak, S., and Šantek, B. "Bioethanol Production from Renewable Raw Materials and Its Separation and Purification: A Review", *Food Technol. Biotechnol.*, vol. 56, no. 3, p. 289, Sep. 2018, doi: 10.17113/ftb.56.03.18.5546.

[7] Tse, T. J., Wiens, D. J., and Reaney, M. J. T. "Production of Bioethanol: A Review of Factors Affecting Ethanol Yield," *Fermentation*, vol. 7, no. 4, p. 268, Nov. 2021, doi: 10.3390/fermentation7040268.

[8] Sanusi, I. A., Suinyuy, T. N., Lateef, A., and Kana, G. E. B. "Effect of nickel oxide nanoparticles on bioethanol production: Process optimization, kinetic and metabolic studies", *Process Biochem.*, vol. 92, pp. 386–400, May 2020, doi: 10.1016/j.procbio.2020.01.029.

[9] Sanusi, I. A., Suinyuy, T. N., Lateef, A., and Kana, G. E. B. "The emerging role of nanotechnology in ethanol production", *Nanotechnology for Biorefinery*, Elsevier, pp.

235–256, 2023, doi: 10.1016/B978-0-323-95965-0.00001-9.

[10] Dutta, S., Saravanabhupathy, S., Anusha, Rajak, R. C., Banerjee, R., Dikshit, P. K., Padigala, C. T., Das, A. K., and Kim, B. S. "Recent developments in lignocellulosic biofuel production withnanotechnological intervention: An emphasis on ethanol", *Catalysts*, vol. 13, no. 11, p. 1439, Nov. 2023, doi: 10.3390/catal13111439.

[11] Shahbaz, A., Hussain, N., Saleem, M. Z., Saeed, M. U., Bilal, M., and Iqbal, H. M. N. "Nanoparticles as stimulants for efficient generation of biofuels and renewables", *Fuel*, vol. 319, no. 123724, p. 123724, Jul. 2022, doi: 10.1016/j.fuel.2022.123724.

[12] Kumar, Y., Yogeshwar, P., Bajpai, S., Jaiswal, P., Yadav, S., Pathak, D. P., Sonker, M., and Tiwary, S. K. "Nanomaterials: stimulants for biofuels and renewables, yield and energy optimization", *Mater. Adv.*, vol. 2, no. 16, pp. 5318–5343, 2021, doi: 10.1039/d1ma00538c.

[13] Ampah, J. D., Yusuf, A. A., Agyekum, E. B., Afrane, S., Jin, C., Liu, H., Fattah, I. M. R., Show, P. L., Shouran, M., Habil, M., and Kamel, S. "Progress and Recent Trends in the Application of Nanoparticles as Low Carbon Fuel Additives-A State of the Art Review", *Nanomaterials (Basel)*, vol. 12, no. 9, Apr. 2022, doi: 10.3390/nano12091515.

[14] Gupta, K., and Chundawat, T. S. "Zinc oxide nanoparticles synthesized using Fusarium oxysporum to enhance bioethanol production from rice-straw", *Biomass Bioenergy*, vol. 143, no. 105840, p. 105840, Dec. 2020, doi: 10.1016/j.biombioe.2020.105840.

[15] Attia, Y., Abdelsalam, E., Saeed, S., Saleh, M., and Samer, M. "Bioethanol production from potato peels using Saccharomyces cerevisiae treated with ZnO and ZnO/g-C3N4 nanomaterials", *Egypt. J. Chem.*, Jun. 2022, doi: 10.21608/EJCHEM.2022.118978.5351.

[16] Koppram, R., Nielsen, F., Albers, E., Lambert, A., Wännström, S., Welin, L., Zacchi, G., and Olsson, L. "Simultaneous saccharification and co-fermentation for bioethanol production using corncobs at lab, PDU and demo scales", *Biotechnol. Biofuels*, vol. 6, no. 1, p. 2, Jan. 2013, doi: 10.1186/1754-6834-6-2.

[17] Nduka, F. O., Onwurah, I. N. E., Obeta, C. J., Nweze, E. J., Nkwocha, C. C., Ujowundu, F. N., Eje, O. E., and Nwigwe, J. O. "Effect of nickel oxide nanoparticles on bioethanol production by IFM 53048 using banana peel waste substrate", *Environ. Technol.*, pp. 1–20, May 2023, doi: 10.1080/09593330.2023.2215450.

[18] Sanusi, I. A., Faloye, F. D., and Gueguim Kana, E. B. "Impact of various metallic oxide nanoparticles on ethanol production by Saccharomyces cerevisiae BY4743: Screening, kinetic study and validation on potato waste", *Catal. Letters*, vol. 149, no. 7, pp. 2015–2031, Jul. 2019, doi: 10.1007/s10562-019-02796-6.

[19] Mayoral, M. C., Izquierdo, M. T., Andrés, J. M., and Rubio, B. "Different approaches to proximate analysis by thermogravimetry analysis", *Thermochim. Acta*, vol. 370, no. 1–2, pp. 91–97, Apr. 2001, doi: 10.1016/S0040-6031(00)00789-9.

[20] Kamran, M. "Energy sources and technologies", *Fundamentals of Smart Grid Systems*, Elsevier, pp. 23–69, 2023, doi: 10.1016/B978-0-323-99560-3.00010-7.

[21] Walkley, A., and Black, I. A. "An examination of the degtjareff method for determining soil organic matter, and a proposed modification of the chromic acid titration method", *Soil Sci.*, vol. 37, no. 1, pp. 29–38, Jan. 1934, doi: 10.1097/00010694-193401000-00003.

[22] Lavudi, S., Oberoi, H. S., and Mangamoori, L. N. "Ethanol production from sweet sorghum bagasse through process optimization using response surface methodology", *3 Biotech*, vol. 7, no. 4, Aug. 2017, doi: 10.1007/s13205-017-0863-x.

[23] Shadangi, K. P., Sarangi, P. K., and Behera, A. K. "Characterization techniques of biomass", *Bioenergy Engineering*, Elsevier, pp. 51–66, 2023, doi: 10.1016/B978-0-323-98363-1.00022-3.

[24] Goutam, S. P., Yadav, A. K., and Das, A. J. "Coriander Extract Mediated Green Synthesis of Zinc Oxide Nanoparticles and Their Structural, Optical and Antibacterial Properties", *Journal of Nanoscience and Technology*, vol. 3, no. 1, pp. 249–252, Oct. 2017. Accessed: Feb. 27, 2024. [Online]. Available: https://www.jacsdirectory.com/journal-of-nanoscience-and-technology/admin/issues/20171002062314_3-1-05%20J NST17079%20Published.pdf.

[25] Hartanto, D., Pambudi, A. B., Cahyanti, D. N., and Utomo, W. P. "On the synthesis of ZSM-5 directly from kaolin bangka with aging time", *IOP Conf. Ser. Mater. Sci. Eng.*, vol. 588, no. 1, p. 012039, Aug. 2019, doi: 10.1088/1757-899X/588/1/012039.

[26] Taranu, B.-O., Novaconi, S. D., Ivanovici, M., Gonçalves, J. N., and Rus, F. S. "A-MnO2 nanowire structure obtained at low temperature

with aspects in environmental remediation and sustainable energy applications", *Appl. Sci.*, vol. 12, no. 13, p. 6821, Jul. 2022, doi: 10.3390/app12136821.

[27] Efeovbokhan, V. E., Egwari, L., Alagbe, E. E., Adeyemi, J. T., and Taiwo, O. S. "Production of bioethanol from hybrid cassava pulp and peel using microbial and acid hydrolysis", *BioResources*, vol. 14, no. 2, pp. 2596–2609, Feb. 2019, doi: 10.15376/biores.14.2.2596-2609.

[28] Zhang, F., Chen, X., Wu, F., and Ji, Y. "High adsorption capability and selectivity of ZnO nanoparticles for dye removal", *Colloids Surf. A Physicochem. Eng. Asp.*, vol. 509, pp. 474–483, Nov. 2016, doi: 10.1016/j.colsurfa.2016.09.059.

[29] Kheiralla, A. F., El-Awad, M., Hassan, M. Y., Hussen, M. A., and Osman, H. I. "Effect of Ethanol/Gasoline Blends on Fuel Properties Characteristics of Spark Ignition Engines", *University of Khartoum Engineering Journal (UofKEJ)*, vol. 1, no. 2, pp. 22–28, Oct. 2011. Accessed: Feb. 27, 2024. [Online]. Available: https://www.academia.edu/16929932/Effect_of_Ethanol_Gasoline_Blends_on_Fuel_Properties_Characteristics_of_Spark_Ignition_Engines

[30] D02 Committee, "Test method for density, relative density, or API gravity of crude petroleum and liquid petroleum products by hydrometer method", *ASTM International, West Conshohocken, PA*, 2008. doi: 10.1520/d1298-99.

[31] Muhaji, and Sutjahjo, D. H. "The characteristics of bioethanol fuel made of vegetable raw materials", *IOP Conf. Ser. Mater. Sci. Eng.*, vol. 296, p. 12-19, Jan. 2018, doi: 10.1088/1757-899X/296/1/012019.